Journal of Thermal Analysis and Calorimetry, Vol. 91 (2008) 1, 17–27

STUDY OF DETERIORATION OF HISTORICAL PARCHMENTS BY VARIOUS THERMAL ANALYSIS TECHNIQUES COMPLEMENTED BY SEM, FTIR, UV–VIS–NIR AND UNILATERAL NMR INVESTIGATIONS

Elena Badea[1*], *Lucreţia Miu*[2], *P. Budrugeac*[3], *Maria Giurginca*[4], *A. Mašić*[1], *Nicoleta Badea*[4] *and G. Della Gatta*[1**]

[1]Department of Chemistry IFM, University of Turin, via P. Giuria 9, 10125 Turin, Italy
[2]National Research and Development Institute for Textile and Leather, str. Ion Minulescu 93, 031215 Bucharest, Romania
[3]National Institute for Research and Development in Electrical Engineering ICPE-CA, Splaiul Unirii 313, 030138 Bucharest, Romania
[4]University 'POLITEHNICA' of Bucharest, str. Polizu 1, 011061, Bucharest, Romania

A comprehensive investigation has been made of a set of 14th to 16th-century parchment bookbindings from the Historical Archives of the City of Turin. Advanced physico-chemical techniques, such as thermal analysis (DSC, TG and DTA), spectroscopy (FTIR and UV-Vis-NIR), scanning electron microscopy (SEM) and unilateral nuclear magnetic resonance (NMR-ProFiler) were employed to assess specific deterioration processes occurring at different levels in the hierarchical structure of parchment. Changes in the measured physical and chemical parameter values of parchment due to interaction with the environment were used to identify possible deterioration pathways.

Keywords: *deterioration pathways, DSC, DTA, FTIR, historical parchments, NMR, SEM, TG, thermal analysis, UV-Vis-NIR*

Introduction

Parchment is a complex material based on collagen, one of the most versatile proteins, whose properties result from its supramolecular structure and hierarchical arrangements from molecules to fibres [1–5]. Parchments' inhomogeneous nature and the influence of external factors as environmental pollution, harsh cleaning, improper conservation and restoration, makes rather difficult the investigation of its ageing and deterioration. Study of the specific deterioration processes in parchments requires a systematic, multidisciplinary approach based on advanced physical-chemical techniques able to collect the maximum amount of information from very small samples. However, correlation between deterioration mechanisms and phenomenological features of damage cannot readily be established since deterioration affects the entire structure of collagen [6, 7].

The measurable physical-chemical and structural properties of parchments have proved useful in the quantitative evaluation of deterioration [8–10] and for the drafting of damage assessment protocols. We have elaborated thermodynamic [11, 12], morphological [13] and molecular [14] markers and criteria for the assessment of damage caused by ageing. The results of accelerated ageing experiments have enabled a distinction to be drawn between four classes of damage, namely no damage, minor, medium and major damage [15], and have provided conservators with a new approach to damage assessment. In addition, kinetic analysis of decomposition processes have been applied to thermoanalytical data (DSC and TA-MS) to predict the thermal stability of undamaged and artificially aged parchment by Roduit and Odlyha [16].

The present study was conducted on a set of 14th to 16th-century parchment bookbindings owned by the Historical Archives of the City of Turin. Thermal analysis results have been correlated with those provided by FTIR, UV-Vis-NIR, SEM and unilateral NMR. It adds to the recent review on thermal analysis techniques (TG, DTG, DTA, DSC and MTA) applied to the study of cultural heritage such as mortars, grounds, sculptures and bricks, painting materials, drying oils [17].

Experimental

Materials

Selected samples were taken from the outer covers, flaps and edges of bookbindings of the 'Collection V'

* On leave from the Faculty of Chemistry, University of Craiova, Calea Bucureşti 165, Craiova 1100, Romania
** Author for correspondence: giuseppe.dellagatta@unito.it

1388–6150/$20.00

Akadémiai Kiadó, Budapest, Hungary
Springer, Dordrecht, The Netherlands

Table 1 List of the parchments

New parchments			
Supplier	Animal	Date	Symbol
NRDITL	Goat	2004	Ref.
Old parchments			
Origin	Type	Date	Symbol
Historical archives of the city of Turin, 'Collection V'	Front cover flap	1375	TO7-1
	Back cover edge	1375	TO7-2
	Front cover	1415	TO8-1
	Front cover flap	1415	TO8-2
	Front cover	1428	TO9-1
	Front cover flap	1428	TO9-2

(Finances, Land Registers, etc.) in the Historical Archives of the City of Turin. Some samples (Table 1) were regarded as representative of the state of conservation of the entire collection.

The parchments used as reference were from goatskin, in accordance with the type of our samples, and were prepared by traditional methods at the National Research and Development Institute for Textile and Leather of Bucharest.

Methods

Differential scanning calorimetry

(*i*) DSC measurements on 'as received' samples were performed in the temperature range 20 to 280°C, at 10°C min^{-1} heating rate in both static air atmosphere and dry nitrogen flow (20 mL min^{-1}) in open aluminium crucibles. Samples were analysed in a dry condition after a few days' storage in a controlled environment (approximately 20°C and 50% RH). Measurements were made in the laboratories of ICPE-CA, Bucharest, and Department of Chemistry IFM, Torino, with a NETZSCH DSC 204 F1 Phoenix and a Setaram DSC 111 calorimeter, respectively.
(*ii*) DSC measurements on 'wet' samples were made from 25 to 110°C, at 10°C min^{-1} heating rate with the NETZSCH calorimeter. Following the addition of 35 μL water, the aluminium crucibles were hermetically sealed and left for 24 h at room temperature to assure reproducible swelling conditions.
(*iii*) DSC measurements in 'excess water' were performed with a SETARAM MicroDSC III calorimeter, from 5 to 95°C, at 0.5°C min^{-1} heating rate. Samples were first kept in 0.5 M acetate buffer solution (pH=5.0) in the calorimetric cell for 2 h at 5°C to assure reproducible hydration conditions.

Simultaneous TG, DTG and DTA analysis

TG, DTG and DTA plots were simultaneously recorded with a NETZSCH STA 409PC apparatus from 20 to 900°C, at 10°C min^{-1} heating rate. Measurements were made in static air atmosphere using α-Al_2O_3 crucibles.

The sample masses were 2 to $4 \cdot 10^{-3}$ g, and 4 to $6 \cdot 10^{-3}$ g for DSC and simultaneous TG-DTG-DTA, respectively.

Micro Hot Table

Parchment fibre shrinkage temperatures were determined by the Micro Hot Table (MHT) method as described in [18]. A Caloris micro hot table controlled by a temperature processor coupled with a stereo microscope Wild Heergbrugg (magnification ×50) assisted by a home-made software was used.

FTIR and UV-Vis-NIR analysis

FTIR spectra in the 4000–400 cm^{-1} wavenumber range were recorded with a Jasco FTIR-620 spectrophotometer equipped with a DLATGS detector and a KBr beam splitter. Samples were prepared by grinding about 1 mg parchment with KBr and pressing the mixture into very thin disks. The maximum resolution of measurements was 1 cm^{-1} [14].

UV-Vis-NIR spectra in the 200–2000 nm wavelength range were obtained with a Jasco V570 double-beam spectrophotometer using diffuse reflection technique and 2 nm resolution.

Changes in sample colour by comparison with a reference new parchment were also evaluated with the CIE-Lab software (CIE-Lab.DIN 6174-976. Testing the chromatic characteristics).

Scanning electron microscopy

SEM observations were made at 5 to 30 kV accelerating voltage with a Leica 420 Stereoscan apparatus equipped with a tungsten filament as described in [12, 13]. Samples were short-pulse coated with graphite to avoid damage due to overheating and analysed on their flesh side at increasing magnifications (×250–×2000).

Unilateral nuclear magnetic resonance

Water ^1H nuclear spin relaxation time measurements were performed with a mobile NMR device (NMR ProFiler, Bruker BioSpin) [19]. The peculiar

features of this device (permanent magnet of 0.5 T, radio frequency field spread a few millimeters from the surface) allow the acquisition of NMR relaxometric data by simply placing the magnet on a parchment. The spin-lattice relaxation time (T_1) was measured because of its higher sensitivity to the water collagen interactions that depend on the deterioration of collagen. The experimental signal intensity was exponentially fitted to derive T_1 values. A 4-hour measurement allows a fitting uncertainty of about ±1 ms.

Results and discussion

Thermal analysis of historical collagen-based materials has not yet been systematically attempted, even though much has been learned about the thermal denaturation of molecular collagen from various biological tissues. Few studies have been made on fibrous collagen within parchments [11–16, 18–20]. Parchment, in fact, mostly (>90%) consists of fibrillar collagen embedded in a hydrated matrix of proteoglycans, mucopolysaccharides, elastin, salts and lipids. This complexity makes it hard to understand how all these components interact and influence one another during the physical and chemical alterations induced by ageing. Since hydration plays a significant rôle in regulating a parchment's response to heating [21–23], we have performed DSC measurements on 'as received' and 'wet' samples, and in 'excess water'. 'As received' samples were also analysed by simultaneous TG, DTG and DTA.

Differential scanning calorimetry

Parchments 'as received'

DSC curves obtained on 'as received' new parchment in both static air and nitrogen flow (Fig. 1) display two endothermic processes. The broad endotherm (I) ranging from room temperature to about 120°C was attributed to loss of the free water content. It overlaps the specific denaturation endotherm which occurs at about 120°C [12]. The small endothermic sharp peak (II) at about 230°C can be related to melting of the stable crystalline fraction of parchment. Process II was first observed for the collagen fibres of steer Achilles tendon and ascribed to the existence of three collagen fractions with different structure and thermal stability, namely the amorphous fraction, and less oriented unstable and stable crystalline fractions [24]. It has since been shown, mainly by X-ray diffraction, that fibrillar collagen I from biological tissues [25] and parchments [26] forms intermixed crystalline and amorphous structures. The stable crystalline fraction is usually characterised by very narrow melting

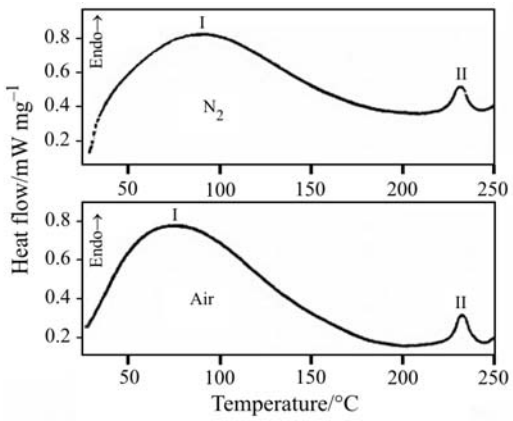

Fig. 1 DSC curves obtained for new parchments 'as received' in dry nitrogen flow and static air atmosphere, respectively. Large peak I represents loss of humidity overlapping the endothermic evidence of denaturation. Small peak II is related to melting of the parchment crystalline fraction

temperatures, whereas the unstable crystalline fraction is associated with a wider range. DSC evidence of melting of the stable crystalline fraction has been found for gelatine [24] and pure collagen, as well as for both recently manufactured and old leathers [27]. We observed a sharp melting peak for all new and old parchments near 230°C in nitrogen flow, whereas in static air atmosphere, the bookbindings, except TO7-1, displayed additional peaks (Table 2) attributable to both the heterogeneity of the aged material and oxidative susceptibility of the random fragmented fibrillar matrix.

'Wet' parchments

We employed DSC on wet samples to determine the hydrothermal stability of parchment [28, 29]. The average onset temperature of the DSC denaturation peak (Fig. 2) was in excellent agreement with the average shrinkage temperature, T_s, measured by MHT for both new and old parchments (Table 3). The differences between the DSC and MHT values observed for some old bookbindings (Table 3, columns 5 and 6) should be attributed to their increased heterogeneity enhanced by difference in sampling, single fibres (MHT) against bulk samples (DSC). Since historical parchments are highly heterogeneous and T_s value characterises the collagen fraction with the lowest hydrothermal stability, further quantitative (denaturation enthalpy) and qualitative (DSC peak components) information provided by DSC measurements offer an objective method to evaluate the heterogeneity of hydrothermal stability of old bookbindings.

Table 2 Thermodynamic parameter values for the melting of the stable crystalline fraction measured by DSC using open crucibles

Sample	Static air atmosphere			Nitrogen flow		
	N	T_{max}/°C	ΔH/J g^{-1}	*N*	T_{max}/°C	ΔH/J g^{-1}
Reference*	1	230±3*	7±2*	1	230±4*	6±2*
TO7-1	1	230.7	10.5	1	232.1	6.4
TO7-2	3	137.6	0.5	1	230.4	6.2
		162.8	0.3			
		228.4	8.8			
TO8-1	2	161.4	0.8	1	236.8	7.4
		238.1	3.4			
TO8-2	3	98.5	1.0	2	97.5	1.0
		159.0	0.4		231.9	5.8
		231.7	2.3			
TO9-1	2	166.3	1.1	2	129.8	1.7
		228.9	1.7		228.1	4.9
TO9-2	2	157.8	0.2	1	232.0	8.0
		232.4	5.7			

*Average values calculated for eight new manufactured parchments (uncertainties are twice standard deviations of the mean).
N=number of DSC peaks corresponding to melting

Parchment in 'excess water' condition

DSC of dry parchments, in fact, only provides a bulk response concerning the fibrous tissue also dependent on the moisture content while wetting gives rise to randomly swollen fibres whose denaturation occurs in a broad temperature range with an onset temperature that practically coincides with the shrinkage temperature. An excess water milieu ensures full and reproducible hydration of samples and provides more comprehensive and accurate values of the thermodynamic parameters associated to thermal denaturation. In excess water, impairment of the fibrillar structure is enhanced and the DSC peaks give more detailed information about damage processes and their features (Fig. 3) [12]. Table 4 sets out the values of these parameters, namely maximum peak temperature, T_d, peak half width, $\Delta T_{1/2}$, maximum peak height, $C^{ex}_{p(max)}$, and enthalpy of denaturation, $\Delta_d H$, for new and old parchments. As shown in Fig. 3a, thermal denaturation of new parchments in excess water displays sharp peaks with a smoothed shoulder on their descending part. This feature has been attributed to the presence of collagen fractions with dissimilar thermal stability [30, 31]. Collagen fibrils inhomogeneously structured with a relatively hard shell and softer, less dense core observed by atomic force microscopy have been attributed to a higher crosslink level near their surface [32]. We have found that artificial ageing induces specific alteration of these two components of collagen and makes the multiple features of DSC curves more evident [33].

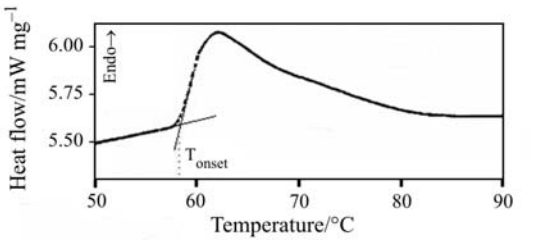

Fig. 2 DSC curve obtained for a new parchment in 'wet' condition and static air atmosphere. The onset temperature, T_{onset}, is practically coincident with the temperature of shrinkage, T_s, measured by MHT

Due to the collagen inhomogeneous structure and cooperative character of its breakdown ageing may be expected to result in a progressively lower and broader energy distribution of its components with different thermal, mechanical and organisation features. In fact, old parchments have frequently displayed widely distributed denaturation temperatures and small endothermic deviations in the range 20 to 40°C (Fig. 3b, curve 2), as well as just before the denaturation peak due to differences in the quality of their collagen fractions provoked by ageing [34]. The DSC curves of the old bookbindings (Fig. 4) displayed different responses to heating and indicated that ageing of external covers (TO8-1 and TO9-1), flaps (TO7-1, TO8-2 and TO9-2) and an edge (TO7-2) has followed different patterns. DSC denaturation peaks of flaps were rather narrow, but very short by comparison with the reference one and displayed higher T_d values (Table 4). Moreover, the

Table 3 Comparison between T_s values determined by both DSC on 'wet samples' and MHT for new (samples N-1 to N-8) and old parchments (RO-1 and RO-2 are 16th-century Romanian documents)

New parchments	T_s/°C		Old parchments	T_s/°C	
	MHT	DSC		MHT	DSC
N-1	55.4	56.3	TO7-1	43.7	46.8
N-2	56.4	58.3	TO7-2	51.5	49.4
N-3	59.9	58.4	TO8-1	56.4	54.4
N-4	56.5	57.8	TO8-2	55.5	59.1
N-5	54.7	52.8	TO9-1	58.7	59.9
N-6	61.2	60.8	TO9-2	52.5	53.8
N-7	57.4	56.6	RO-1	52.5	53.8
N-8	61.1	63.0	RO-2	56.3	57.0
Average	57.8±2.6	58.0±3.0			

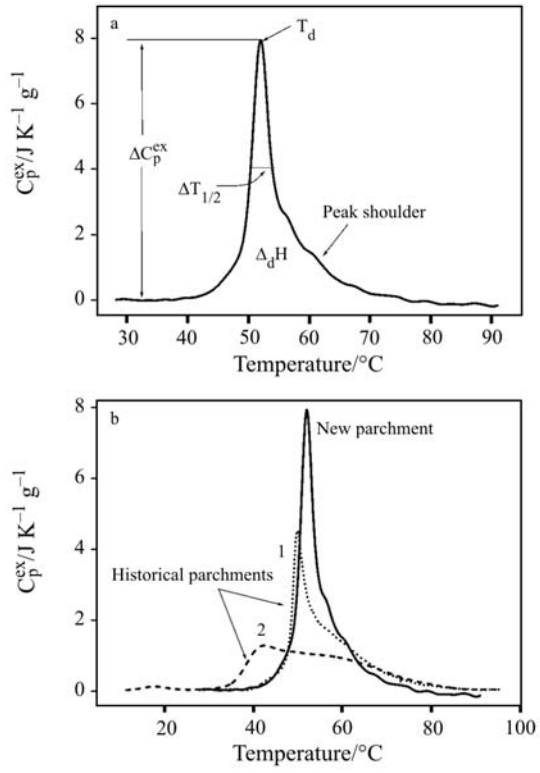

Fig. 3 a – DSC curve for new parchment in 'excess water' and the derived thermodynamic parameter values; b – DSC curves of two historical parchments: (1) bookbinding damaged by the 1966 flood from the State Archive of Florence; (2) single sheet document dated 1832 from the National Archives of Stirling

peak shoulder is spread over a wider temperature range and its contribution to $\Delta_d H$ is increased by comparison with the reference. Very small endothermic deviations were detected both before 40°C and DSC peak onset. TO8-2 displayed a clear and broad endotherm in the 20 to 40°C range. The sample taken from the back cover edge, TO7-2, gave an even broader and lower peak with an evident

Table 4 Thermodynamic parameter values for thermal denaturation measured by DSC 'in excess water'

Sample	T_d/ °C	$\Delta_d H$/ J g^{-1}	$\Delta T_{1/2}$/ °C	$C^{ex}_{p(max)}$/ J K^{-1} g^{-1}
Ref.*	52.7±0.9	48±4	4.0±0.6	8.3±1.4
TO7-1	55.7	30.2	4.8	3.0
TO7-2	53.2	25.8	6.3	1.9
TO8-1	50.7	22.8	29.1	1.1
TO8-2	53.8	29.3	6.0	1.9
TO9-1	53.0	22.1	12.3	1.3
TO9-2	55.6	26.9	4.8	2.6

*Average values calculated for eight new manufactured parchments (uncertainties are twice standard deviations of the mean)

and broad endotherm in the range 20 to 40°C. DSC peaks for the two external covers, TO8-1 and TO9-1, were further broader and lower with $\Delta_d H$ values less than 50% by comparison to the reference (Table 4). T_d values higher than the reference are rather frequent for old bindings, and are probably due to a cross-link formation prior to deterioration through polypeptide chain cleavage [12, 15]. $\Delta T_{1/2}$ values, in fact, which are directly correlated with the structural heterogeneity of parchment, increased by comparison with the reference from 120 (flaps) to 150 (edge) and 700% (covers).

The study of artificially aged parchments showed that dampness combined with a relatively high temperature results in a progressively greater contribution of the shoulder to the enthalpy of denaturation, $\Delta_d H$ [15]. On the other hand, the presence of acid species, such as HNO_2^- and HNO_3^- and HSO_3^- produced by exposure to NO_x and SO_2, promotes hydrolysis of the stable fraction (i.e. that giving the shoulder) and reduces this contribution [15, 33]. The occurrence of small and broad endo-

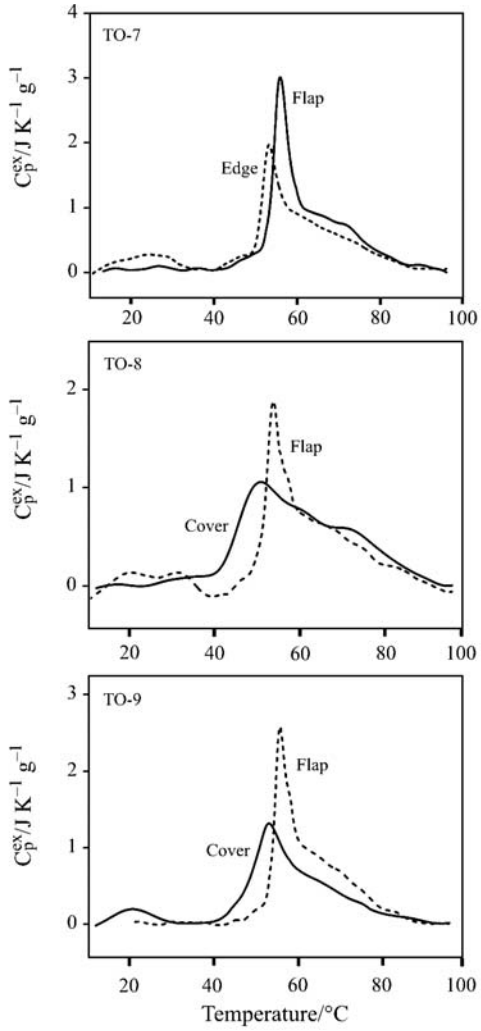

Fig. 4 DSC curves in 'excess water' for old bookbindings displaying denaturation peaks and further endothermic evidences at temperatures lower than T_d

therms in the range 20 to 40°C was related to collagen gelatinisation and the less sharp onset of the DSC peak was assigned to the transition of a disordered fraction of collagen [12]. All these features are present in the DSC peaks of old bookbindigs and their intensity depends on the type (cover, flap or edge) of sample.

Simultaneous TG, DTG and DTA analysis

Figure 5 shows typical TG, DTG and DTA curves of a new parchment displaying a four-step thermal degradation in air where each step is accompanied by specific mass loss [11, 27, 35–39]. In the first endothermic step (I) at around 100°C, the moisture content of parchments is lost. The next two steps are exothermic and consist in the thermo-oxidation (II) and pyrolytic decomposition (III) at about 300 and 550°C, respectively. The last step (IV) was attributed

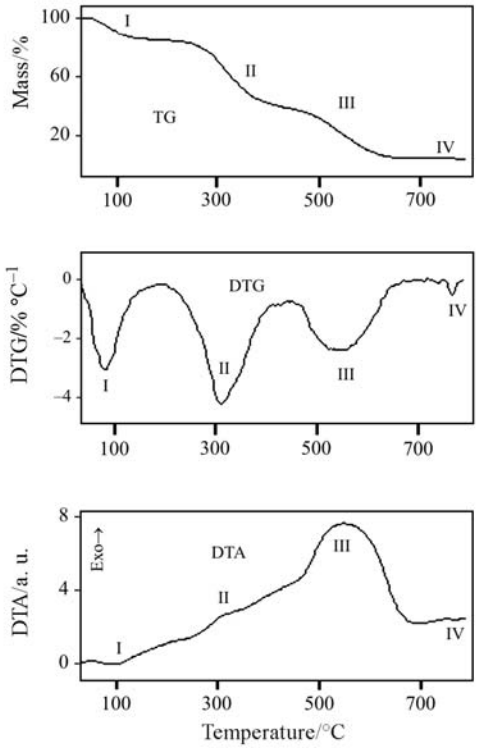

Fig. 5 TG, DTG and DTA curves showing the four-step non-isothermal degradation in air for a new parchment

to the decomposition of the small quantity of $CaCO_3$ usually present in parchments.

The average values of the temperatures corresponding to the maximum reaction rate, T_{min}^{DTG}, for steps II and III, and mass loss evaluated from TG and DTG curves, are presented in Table 5. New parchments always displayed average T_{min}^{DTG} and $\%\Delta m$ values higher than old parchments. Since the temperature corresponding to the maximum rate of step II was in the range 309.8 to 328.4°C, we have compared the dm/dt values of new and old parchments at 310, 315, 320 and 325°C (Table 6). New parchments always displayed higher dm/dt values than old parchments. A similar thermal behaviour observed for new and old leather was attributed to the presence of reactive sites introduced by tanning and progressively lost on ageing [11, 39]. The lower thermo-oxidation rate of old bookbindings could be attributable to their high heterogeneity caused by the splitting off and consequent oxidative breakdown of fibrils.

FTIR and UV–Vis–NIR analysis

FTIR analysis was employed to investigate the secondary structure of collagen since marker bands explored in detail by mid-IR spectroscopy permit the identification and quantification of ageing-induced changes at the molecular level of collagenous materials [14, 15, 33]. NIR spectroscopy is also useful

Table 5 Thermal degradation behaviour of new and old parchments from mass loss (steps I to III and total) and T_{min}^{DTG} (steps II and III) values

Sample	Mass loss/%				T_{min}^{DTG}/°C	
	Step I	Step II	Step III	Total	Step II	Step III
New parchments (8 samples)	16.4±0.9	45.6±0.9	36.4±1.3	98.8±1.0	318.2±5.6	561.9±15.7
Old parchments	13.5±1.8	40.2±2.5	33.4±2.3	87.1±5.4	312.6±3.1	532.4±17.0

Table 6 Comparison between d*m*/d*t* values for new and old parchments in the temperature range corresponding to the maximum rate of step II (310, 315, 320 and 325°C)

Sample	d*m*/d*t*/% min^{-1}			
	310°C	315°C	320°C	325°C
New parchments (8 samples)	4.03±0.16	4.09±0.11	4.13±0.07	4.10±0.16
Old parchments	3.72±0.06	3.71±0.07	3.65±0.08	3.56±0.08

for the qualitative analysis of a complex material such as parchment. Nonetheless, spectrum-structure correlations have not been well established for collagenous materials in the NIR region.

In Fig. 6, FTIR spectra of a new parchment and old bookbindings are compared. The main features of the spectra considered for the evaluation of deterioration are the strong and broad band centred at 3450 cm^{-1}, assigned to the stretching of both OH and NH groups variously hydrogen bonded, the amide I doublet near 1655 cm^{-1} (C=O stretching) and the amide II band at 1544 cm^{-1} (N–H bending) [40]. The amide II band shift corresponding to an increase in the separation of the amide I and II bands indicates the helix-coil conversion, i.e. collagen to gelatine [41]. Moreover, the amide I band, mainly associated to the stretching vibrations of carbonyl groups along the peptide backbone, provides a very sensitive marker of collagen secondary structure. Hydrolytic cleavage of both collagen and gelatine is indicated by an increase in the OH stretching or bending frequencies at 3400 and 1650 cm^{-1}, respectively [15] which gives rise to an intensity increase of the amide I band. Oxidation of the polypeptidic chains results in formation of carbonyl compounds which give rise to a band in the 1700–1750 cm^{-1} region [41]. The relative positions and intensities of these bands can be of assistance in the identification and measurement of specific deterioration pathways in parchments [40–42]. The ratio between amide I and amide II bands, AI/AII, indicates the hydrolysis degree of the polypeptidic chains, whereas their position difference, $\Delta\nu$, is related to collagen denaturation (Table 7). The band intensities of hydroxyl and carbonyl groups normalised to the amide I intensity are also listed in Table 7. The values reported suggest that collagen from covers (TO8-1 and TO9-1) is more

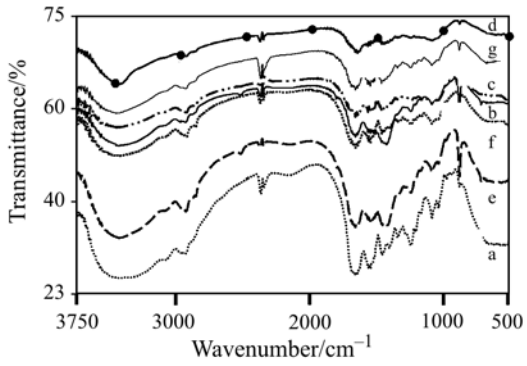

Fig. 6 FTIR spectra of new and old parchments: a – reference; b – TO9-2; c – TO9-1; d – TO7-1; e – TO7-2; f – TO8-1; g – TO8-2

Table 7 Amide I and II bands relative intensities and positions as well as the relative band intensities of hydroxyl and carbonyl groups normalised to the amide I intensity

Sample	AI/AII	$\Delta\nu$	A_{OH}/AI	A_{CO}/AI
Ref.*	1.004	101	1.068	–
TO7-1	1.024	112	1.064	–
TO7-2	1.041	121	1.040	1.160
TO8-1	1.050	93	1.240	–
TO8-2	1.032	111	1.054	1.235
TO9-1	1.024	104	1.153	–
TO9-2	0.987	112	1.084	–

*Average values

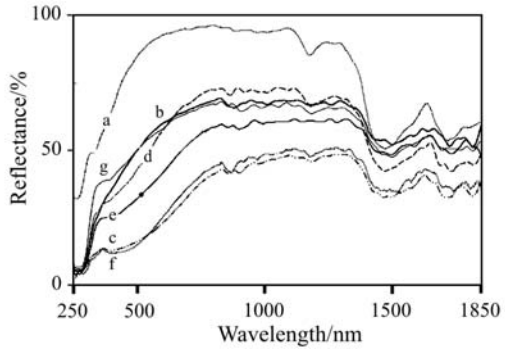

Fig. 7 UV–Vis–NIR spectra of new and old parchments: a – reference; b – TO9-2; c – TO9-1; d – TO7-1; e – TO7-2; f – TO8-1; g – TO8-2

hydrolysed, whereas collagen from the cover edge (TO7-2) is mainly affected by oxidation and denaturation. The amide II shift towards lower frequencies observed for the flap TO7-1 is also a marker of denaturation.

In Fig. 7, UV–Vis–NIR spectra of old bookbindings compared with a new reference parchment spectrum are presented. The main absorption peaks detected in the measurement range 200–2000 nm are listed in Table 8. All samples showed absorption in the range 250–290 nm. TO8-1 and TO9-1 also displayed bands at 390 and 434 nm, respectively. The absorption peaks in the bandwidth 250–400 nm are given by $\pi \rightarrow \pi^*$ and $n \rightarrow \pi^*$ transitions of C=O, NH and CONH groups. The NIR region is dominated by the overtone and combination bands of water at around 1450 and 1950 nm, and displays specific bands around 1730 nm due to CH groups in lipids and protein and a weaker band near 1820 nm [40, 43] assignable to the first overtone of CH_3 and CH_2 groups, respectively [43]. Two weak bands appeared clearly around 1500 and 2000 nm and were attributed to the first overtone of the N–H stretching and NH_2 stretching of the $CONH_2$ group of collagen [34].

Table 8 UV–Vis–NIR bands in new and old parchment spectra

Sample	Bands/nm
Reference*	272; 1182; 1490; 1732; 1936
TO7-1	270; 1500; 1724; 1814
TO7-2	284; 400; 1468; 1494; 1724; 1814
TO8-1	260; 276; 390; 1500; 1732
TO8-2	256; 84; 1182; 1470; 1730; 1818
TO9-1	294; 434; 1458; 1726
TO9-2	264; 290; 1458; 1508; 1724

The water band caused by the first overtone of O–H stretching and associated with free water was observed near 1490–1500 nm for new parchments and for TO7-1 and TO8-1, at 1458 nm for TO9-1 and TO9-2 and at 1468–1470 nm for TO7-2 and TO8-2. Although there has been no report on NIR spectra of parchments, NIR spectra of water [44, 45] and proteins have been investigated in detail [46, 47]. According to Segtnan *et al.* [44] and Šašić *et al.* [45] this broad band is assignable to two water species with weaker and stronger hydrogen bonds, namely second-order absorbed water species and first-order absorbed water. Since proteins have two bands near 1400 and 1500 nm due to the combinations of CH vibrations and the first overtone of NH stretching, the feature in the 1490–1510 nm region may be due to the overlapping of bands arising from strongly hydrogen bonded water and collagen [43]. Therefore, the changes observed could be assigned to variations of the free water content of parchments and different states of their hydrogen bonds [48]. The results of the TG experiments, in fact, confirmed the higher free water content of the new parchments (Table 5). As a consequence, the 1450–1510 nm region appears to be very specific for absorption of water and further studies will be made at different values of relative humidity to confirm that moisture sorption is related to the deterioration condition of parchments.

The colour characteristics of bookbindings were measured in the UV–Vis domain and are listed in Table 9. The luminosity variation ΔL^* values indicated that TO7-2 and TO9-2 were most affected by oxidation.

Table 9 Colour characteristics of parchments

Sample	L^*	a^*	b^*	C^*	$H°$	ΔL^*
Reference	95.77	–0.82	8.95	8.99	95.22	–
TO7-1	79.52	0.65	12.75	12.77	87.09	–16.25
TO7-2	51.89	5.73	11.76	13.08	64.01	–43.88
TO8-1	67.70	3.76	12.42	12.97	73.14	–28.07
TO8-2	76.75	3.87	15.64	16.11	76.10	–19.02
TO9-1	50.29	5.30	11.63	12.78	65.51	–45.48
TO9-2	73.18	2.15	18.10	18.23	83.22	–22.59

L^* – luminosity; a^* – red colour; b^* – yellow colour; C^* – croma; $H°$ – colour angle

Scanning electron microscopy

SEM has provided a large collection of local high resolution images of the surface morphology of parchments for assessment of their surface state. For new undamaged parchment, a network of integral collagen fibres with distinct contours and sharp edges (Fig. 8a) was clearly observed on the flesh side, whereas ageing/deterioration resulted in alteration of shape, dimensions and aspect until partial or complete loss of the fibrous network characteristics (Figs 8b to f) [12, 13, 19]. SEM images reported here are solely concerned with the surface of samples and their evaluation is based on our morphological criteria for ranking damage in historical parchments [12, 13, 15, 19]. Nonetheless, SEM observations correlate well with DSC results which essentially refer to bulk properties, e.g. the bundling of collagen fibrils displayed by TO7-1 (Fig. 8e), its high T_d value (Table 4) and single melting peak (Table 2) all assign its high crystallinity and cross-linkage. Moreover, gelatinisation process observed for TO9-1 (glassy layer) and TO7-2 (swollen fibres) is underscored by the presence of small, broad DSC peaks in the range 20 to 40°C (Fig. 4). The information obtained with SEM correlates well with molecular data from spectroscopic analysis, too, e.g. the very fragmented surface observed for TO8-1 sample agrees with its high hydrolysis level indicated by the IR markers.

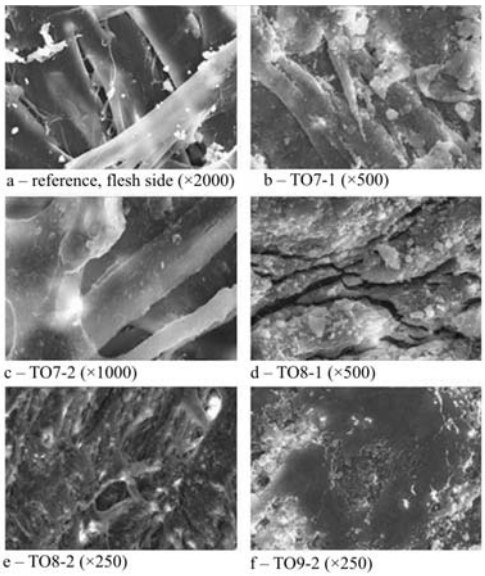

Fig. 8 High magnification SEM images showing typical morphology of old bookbindings by comparison with a new undamaged parchment: a – intact fibre network (flesh side); b – bundled-up fibres; c – swollen and spaced fibres; d – fragmented surface; e – fibres beneath melt-like layer; f – glassy surface

Unilateral nuclear magnetic resonance with an NMR ProFiler

Unilateral NMR is a nondestructive technique used for *in situ* qualitative measurements of alteration of the water environment which can be applied to water within parchments. As a first step, the independency of T_1 values (around 45 ms) on the origin of the new, undamaged parchments was assessed. We have previously found that humid heating results in T_1 shortening, consistent with water interacting with partially gelatinised collagen [15]. Conversely, treatments in atmospheres polluted with NO_x or SO_2 brought out higher T_1 values, as a result of water mobility increase due to the acid hydrolytic cleavage of collagen polypeptide chains [15]. Since the H-bonding ability of a parchment varies with its structural and organisational integrity, aged and deteriorated samples are expected to give rise to proton fractions with different spin-lattice relaxation times. Various T_1 values indicative of different water environments were, in fact, obtained for the old bookbindings (Table 10), in fair agreement with the deterioration pathways deduced from the DSC, SEM and IR results [49].

Table 10 NMR longitudinal relaxation time, T_1, for old bookbindings

Sample	T_1/ms		
	Gelatinized collagen	Swollen collagen	Hydrolyzed collagen
TO7-1		32.5	
TO7-2	*	19.1	
TO8-1	*	18.4	#
TO8-2	*	27.1	
TO9-1	*	15.7	
TO9-2		31.8	

*Short T_1 component revealed. #Long T_1 component revealed

Correlations between the thermal analysis results and data obtained by spectroscopy, SEM and unilateral NMR

It should be stressed that damage to collagen may be variously distributed throughout its hierarchical organisation. The techniques used in this paper give information on specific alterations at different structural levels of parchment whose correlation can account for the progress of deterioration from molecular to fibre level. For example, gelatinisation, frequently found in historical parchments, occurs when the triple helix of collagen molecules unravels to form a random coil. The evolution of deterioration from a fibrous into a gelatine-like state generally

leads to irreversible damage. While the macroscopic assessment of parchment does not detect the occurrence and progress of gelatinisation, our techniques distinguish and localise the level where it manifests. The presence of disordered structures is indicated by high values of IR denaturation marker $\Delta\nu$, by the low $\Delta_d H$ and high $\Delta T_{1/2}$ values, as well as by low spin-lattice relaxation time T_1. Moreover, the glassy surface observed by SEM can be regarded as an early sign of gelatinisation.

Hydrolytic processes are individuated by high AI/AII and A_{OH}/AI ratio values, low hydrothermal stability and high T_1 value. Furthermore, the decrease of hydrothermal stability accompanied by the formation of carbonyl compounds, presence of methionine oxidation derivatives and concomitant reduction of CH_2 and CH_3 stretching contributions [15] should be considered as arising from chemical changes in the peptide chain produced by oxidative breakdown. On the other hand, a high hydrothermal stability, an increased contribution of the DSC peak shoulder to the enthalpy of denaturation and a high degree of crystallinity suggest formation of cross links within the collagen structure. It has been shown that in some cases lipids appear to evince a great degree of crystallinity [50]. Thus, when oxidation markers are also present, specific collagen-lipid interactions may be presumed.

Conclusions

In summary, thermal analysis, and especially DSC measurements, and the other physical-chemical techniques we used examined a number of micro-, meso- and molecular features in parchment. These techniques were employed to evaluate deterioration due to ageing for a series of bookbindings from the Historical Archives of the City of Turin. A number of thermodynamic, chemical and structural markers were proposed to describe the main deterioration pathways.

TO7-2 (back cover edge) has a more heterogenous structure than TO7-1 (flap) as indicated by the melting behaviour of its crystalline fraction (2–3 peaks). DSC peaks shape and parameter values suggested a lower hydrothermal stability for TO7-2 and IR markers indicated its oxidation and denaturation. Earlier gelatinisation of TO7-2 was revealed by DSC in excess water and by SEM, while crosslink formation could be invoked for the more stable TO7-1 sample.

TO8-1 (front cover), appears to be seriously degraded in the light of its very low hydrothermal stability, very high value of DSC peak half-width, low crystallinity and high degree of hydrolysis. TO8-2 (flap) has shown higher level of oxidation and cross-links, but lower denaturation and hydrolysis and appears less deteriorated.

TO9-1 (front cover) has shown a higher degree of hydrolysis and heterogeneity by comparison with TO9-2 (flap) which, on the other hand, has displayed a more extensive denaturation process. Gelatinisation was observed by SEM for TO9-1 and cross-link formation can be supposed for TO9-2, as from its high thermal stability and crystallinity.

In conclusion, our findings pointed to deduce a strong loss and randomisation of the helical structure for outer covers, a higher crosslink formation for flaps and a significant oxidation and gelatinisation for edges.

Acknowledgements

This research was funded by European Union Fifth Framework project EVK4-2001-00067, Improved Damage Assessment of Parchment (IDAP) and by the Italian Piedmont Region project D39, Old Parchment: Evaluating Restoration and Analysis (OPERA). The enthusiastic collaboration of Stefano Benedetto and Anna Braghieri from the Historical Archives of the City of Turin is warmly acknowledged.

References

1 A. Rich and F. H. C. Crick, J. Mol. Biol., 3 (1961) 483.
2 R. D. B. Fraser, T. P. MacRae and E. Suzuki, J. Mol. Biol., 129 (1979) 463.
3 B. Brodsky and E. F. Eikenberry, Method Enzymol., 82 (1982) 127.
4 J. Bella, M. Eaton, B. Brodsky and H. M. Barman, Science, 266 (1994) 75.
5 C. A. Miles and A. J. Bailey, Micron, 32 (2001) 325.
6 T. J. Wess, M. Drakopoulos, A. Snigirev, J. Wouters, O. Paris, P. Fratzl, M. Collins, J. Hiller and K. Nielsen, Archaeometry, 43 (2001) 117.
7 C. J. Kennedy and T. J. Wess, Restaurator, 24 (2003) 61.
8 E. Mannucci, R. Pastorelli, G. Zerbi, C. E. Bottani and A. Facchini, J. Raman Spectrosc., 31 (2000) 1089.
9 A. E. Aliev, Biopolymers, 77 (2005) 230.
10 C. A. Maxwell, T. J. Wess and C. J. Kennedy, Biomacromolecules, 7 (2006) 2321.
11 P. Budrugeac, L. Miu, V. Bocu, F. J. Wortman and C. Popescu, J. Therm. Anal. Cal., 72 (2003) 1057.
12 G. Della Gatta, E. Badea, R. Ceccarelli, T. Usacheva, A. Mašić and S. Coluccia, J. Therm. Anal. Cal., 82 (2005) 637.
13 A. Mašić, E. Badea, R. Ceccarelli, G. Della Gatta and S. Coluccia, in 'Lo Stato dell'Arte 2', Proceedings II Congresso Nazionale IGIIC, Il Prato, Padova 2004, ISBN 88-87243-94-8, pp. 52–57.
14 A. Meghea, M. Giurginca, N. Iftimie, L. Miu, V. Bocu and P. Budrugeac, Mol. Cryst. Liq. Cryst., 418 (2004) 285.
15 G. Della Gatta, E. Badea, A. Mašić and R. Ceccarelli, in 'Improved Damage Assessment of Parchment (IDAP) Collection and Sharing of Knowledge.' Ed. R. Larsen, Directorate-General for Research, Directorate

Environment, European Communities 2007, ISBN 987-92-79-05378-8, pp. 51–60.
16 B. Roduit and M. Odlyha, J. Therm. Anal. Cal., 85 (2006) 157.
17 J. Pires and A. J. Cruz, J. Therm. Anal. Cal., 87 (2007) 411.
18 R. Larsen, D.V. Poulsen and M. Vest, in 'Microanalysis of Parchment', Ed. R. Larsen, Archetype Publications Ltd., London 2002, pp. 55–62.
19 A. Mašić, Doctoral Dissertation: Applicazione di tecniche innovative nello studio dei processi di degrado dei manufatti di interese artistico-culturale, University of Turin, Turin, 2006.
20 D. Fessas, M. Signorelli and A. Schiraldi, Thermochim. Acta, 447 (2006) 30.
21 C. E. Weir, J. Am. Leather Chem. Assoc., 44 (1949) 108.
22 C. Delisi and M. H. Shamos, J. Polym. Sci., 10 (1972) 673.
23 M. Luescher, M. Rueff and P. Schindler, Polymers, 13 (1974) 2489.
24 Y. Okamoto and K. Saeki, Kolloid-Z., Z. Polym., 194 (1964) 124.
25 D. J. Hulmes, T. J. Wess, D. J. Prockop and P. Fratzl, Biophys. J., 68 (1995) 1661.
26 C. J. Kennedy, K. Nielsen, L. Ramsay and T. J. Wess, Fibre Diffr. Rev., 11 (2003) 117.
27 P. Budrugeac, L. Miu and M. Souckova, J. Therm. Anal. Cal., 88 (2007) 693.
28 W. K. Loke and E. Khor, Biomaterials, 16 (1995) 251.
29 C. Chahine, Thermochim. Acta, 365 (2000) 101.
30 P. Kronick, B. Maleeff and R. Carroll, Connect. Tissue Res., 18 (1988) 123.
31 D. G. Wallace, R. A. Condell, J. W. Donovan, A. Paivinen and W. M. Rhee, Biopolymers, 25 (1986) 1875.
32 T. Gutsmann, G. E. Fantner, M. Venturoni, A. Ekani-Nkodo, J. B. Thompson, J. H. Kindt, D. E. Morse, D. Kuchnir Fygenson and P. K. Hansma, Biophys. J., 84 (2003) 2593.
33 R. Larsen, D. V. Poulsen, F. Juchauld, H. Herosch, M. Odlyha, J. de Groot, T. Wess, J. Hill, C. Kennedy, G. Della Gatta, E. Badea, A. Mašić, S. Boghosian and D. Fessas, in Preprints of ICOM Committee for Conservation 14th Triennial Meeting, The Hague, James and James Ed., London 2005, ISBN 1-84407-253-3, Vol. 1, pp. 199–208.
34 E. Badea, A. Mašić, L. Miu, C. Laurora, A. Braghieri, V. E. Marinescu, S. Coluccia and G. Della Gatta, in 'Lo Stato dell'Arte 5', Nardini Editore, Firenze 2007, ISBN 978-88-404-4156-6, pp. 101–108.
35 J. J. Lim and M. H. Shannon, Biopolymers, 13 (1974) 1791.
36 G. de Simone, B. Naviglio, M. Tomaselli, L. Bianchi, D. Sannino and P. Ciambelli, XXIII IULTCS Congress, Friedrichshafen 1995, Part 1, Paper 21.
37 A. Kaminska and A. Siokowska, Polym. Degrad. Stab., 51 (1996) 15.
38 L. F. Lozano, M. A. Pena-Rico, A. Hereira, J. Ocotlan-Flores, A. Gomez-Cortes, R. Velazquez, I. A. Belio and L. Bucio, J. Mater. Sci., 38 (2003) 4777.
39 P. Budrugeac, L. Miu, C. Popescu and F. J. Wortmann, J. Therm. Anal. Cal., 79 (2004) 975.
40 B. Brodsky-Doyle, E. G. Bendit and E. R. Blout, Biopolymers, 14 (1975) 937.
41 M. Derrick, Book and Paper Group Annual, The American Institute for Conservation, Vol. 10, Washington D.C., 1991.
42 A. T. Balaban, M. Banciu and I. Pogany, 'Application of physics methods in organic chemistry', Ed. Ştiinţificăş i Enciclopedică, Bucureşti, 193.
43 H. M. Heise, In Infrared and Raman Spectroscopy of Biological Materials; H. U. Gremlich, B. Yan Eds; Marcel Dekker: New York 2000.
44 V.H. Segtnan, S. Šašić, T. Issaksson and Y. Ozaki, Anal. Chem., 73 (2001) 3153.
45 S. Šašić, V. H. Segtnan and Y. Ozaki, J. Phys. Chem. A, 106 (2002) 760.
46 Y. Wang, K. Murayama, Y. Myojo, R. Tsenkova, H. Hayashi and Y. Ozaki, J. Phys. Chem. B, 102 (1998) 6655.
47 Y. Wu, B. Czarnik-Matsusewicz, K. Murayama and Y. Ozaki, J. Phys. Chem. B, 104 (2000) 5840.
48 M. Egawa, T. Fukuhara, M. Takahashi and Y. Ozaki, Appl. Spectrosc., 57 (2003) 473.
49 A. Mašić, E. Badea, G. Martra and S. Coluccia, Nanoletters, submitted.
50 C. J. Kennedy, J. C. Hiller, D. Lammie, M. Drakopolos, M. Vest, M. Cooper, W. P. Adderley and T. J. Wess, Nanoletters, 4/8 (2004) 1373.

DOI: 10.1007/s10973-007-8513-x